 Cytometry 45:151–157 (2001)

A Flow Cytometry Assay Simultaneously Detects Independent Apoptotic Parameters

Andrea Rasola[1]* and Massimo Geuna[2]

[1]Division of Molecular Oncology, Institute for Cancer Research, University of Torino Medical School, Candiolo, Italy
[2]Laboratory of Tumor Immunology, Institute for Cancer Research, University of Torino Medical School, Candiolo, Italy

Received 5 February 2001; Revision Received 11 July 2001; Accepted 20 July 2001

Background: Apoptosis regulation is of fundamental importance in tissue homeostasis and in the pathogenesis of a variety of diseases. Different cytofluorometric methods are used to investigate apoptotic events. We set up a method to simultaneously evaluate mitochondria depolarization, cell morphology changes, and loss of plasma membrane asymmetry and integrity, thus increasing the information and minimizing errors in the analysis of the apoptotic process.

Methods: Jurkat T cells were induced to undergo apoptosis with different agents. They were labeled with (1) the mitochondrion-selective probes tetramethylrhodamine methyl ester (TMRM) or chloromethyl X-rosamine (CMXRos), which do not accumulate in depolarized mitochondria; (2) Annexin V-fluorescein isothyocianate (FITC) to detect phosphatidylserine (PS) exposure on the cell surface; and (3) propidium iodide (PI) to assess loss of plasma membrane integrity. Cell morphology changes were studied following variations in light scatter parameters.

Results: This is a fast, reliable, and reproducible technique to detect simultaneously independent apoptotic changes by cytofluorometric inspection. TMRM is more effective than CMXRos in responding to variations in the electrochemical gradient of mitochondria.

Conclusions: This technique allows us to integrate the analysis and to follow the kinetics of different apoptotic cell changes. Cytometry 45:151–157, 2001.

Key terms: apoptosis; Annexin V; CMXRos; flow cytometry; lymphocytes; PI; TMRM

Apoptosis is endowed with a sequence of sharply regulated events that culminate in cell death. Cells undergoing the apoptotic process display depolarization of the inner mitochondrial membrane electrochemical gradient ($\Delta\psi_m$), mitochondrial release of apoptogenic molecules, activation of specific proteases termed caspases, blebbing of cytosolic vesicles from the cell surface and loss of plasma membrane asymmetry, condensation of nuclear material, and finally, DNA cleavage and ruptures of the plasma membrane (1–7).

A number of techniques have been developed to investigate the different features of the apoptotic process, ranging from electron microscopy ultrastructural inspections to sophisticated biochemical and cytofluorometric methods. However, some of these cell changes are not specific to the apoptotic process. Therefore, to validate the presence of apoptosis in a cell sample, one single assay is usually not considered sufficient. Nonetheless, pooling data obtained with independent techniques has some disadvantages, especially when investigating subtle changes occurring at particular steps of the apoptotic cascade. For example, the use of independent assays can hamper the interpretation of results by increasing experimental variability. Also, it may be difficult to order the time sequence of closely related steps and it may be impossible to quantify results obtained with some of these techniques.

In order to bypass these problems, we have combined several investigation techniques into one single cytofluorometric assay of apoptosis. Mitochondrial dysfunction was assessed by using mitochondrion-permeable, voltage-sensitive dyes that accumulate in the organelle matrix of healthy cells, but not in the matrix of depolarized mitochondria (8–10). Analysis of cell morphology changes was performed following variations of the forward (FSC) and side light scatter (SSC) parameters (11,12). Plasma membrane alterations were investigated at two different steps: the loss of asymmetry was detected using Annexin V labeled with fluorescein isothiocyanate (FITC), which measures phosphatidylserine (PS) exposure on the cell surface (13); large plasma membrane ruptures were revealed by staining cells with propidium iodide (PI), which

Grant sponsor: Associazione Italiana Ricerca Cancro; Grant sponsor: Progetto Finalizzato Biotecnologie of the Consiglio Nazionale delle Ricerche.

*Correspondence to: Andrea Rasola, Division of Molecular Oncology, Institute for Cancer Research, Strada Provinciale 142, km 3.95, 10060 Candiolo (TO) Italy.

E-mail: arasola@ircc.unito.it

permeates into heavily damaged cells (14). Thus, the same cell sample can be used to visualize early apoptotic events, such as mitochondrial loss of function, mid steps, such as cell shrinkage and PS externalization, and late hallmarks of cell death, such as plasma membrane permeabilization to PI. The apoptotic features of each cell subpopulation were integrated and followed in their ordered appearance.

MATERIALS AND METHODS

Chemicals and Antibodies

Anisomycin, antimycin A, carbonil cyanide m-chlorophenyl-hydrazone (CCCP), mannitol, PI, rotenone, staurosporine, and urea were provided by Sigma (St. Louis, MO). FITC-conjugated Annexin V was provided by Boehringer Mannheim (Indianapolis, IN). Chloromethyl X-rosamine (CMXRos) and tetramethylrhodamine methyl ester (TMRM) were provided by Molecular Probes (Eugene, OR) and the CH11 anti-human Fas monoclonal agonist antibody was provided by Upstate Biotechnology (Lake Placid, NY).

Cell Culture and Apoptosis Induction

Human T-leukemia Jurkat cells were grown in suspension in RPMI 1640 culture medium supplemented with 5% fetal bovine serum (FBS; Gibco BRL, Gaithersburg, MD) and 2 mM L-glutamine in a humidified, 5% CO_2 incubator at 37°C. In order to trigger apoptosis, cells were incubated for 5 h in multiwell tissue culture plates at the seeding density of 2×10^6 cells/ml with anisomycin (500 ng/ml), staurosporine (50–300 nM), or the CH11 anti-Fas agonist antibody (150 ng/ml). Kinetics analysis of apoptosis induction was performed in the time range 30 min to 5 h. Mitochondrial depolarization was achieved by incubating Jurkat cells for 5 h with antimycin A (50 μM), rotenone (50 μM), or CCCP (50 μM) in the same culture conditions as above. Control experiments were performed to exclude solvent (dimethylsulfoxide [DMSO]) nonspecific effects on apoptosis induction. Anisoosmotic conditions were obtained either by adding deionized water to the culture medium to a final osmolarity of 200 mosM (hypoosmotic shock) or by adding 210 mM mannitol or urea to the culture medium (hyperosmotic shock to a final osmolarity of 500 mosM). Each experiment was repeated at least seven times and representative experiments were reported.

Flow Cytometric Analysis of Apoptosis

After induction of apoptosis, 0.5×10^6 cells were washed once in phosphate-buffered saline (PBS) and resuspended in 50 μl HEPES buffer (10 mM HEPES, 135 mM NaCl, 5mM $CaCl_2$). Cells were incubated for 15 min at 37°C in FITC-conjugated Annexin V (following manufacturer's instructions), TMRM (at a final concentration of 200 nM, freshly prepared from stock solution 10 mM in DMSO) or CMXRos (at a final concentration of 200 nM, freshly prepared from stock solution 1 mM in DMSO), and PI (1 μg/ml).

Samples were analyzed on a FACSCalibur flow cytometer (Becton Dickinson, San Jose, CA) equipped with a 15-mW 488-nm argon ion laser. The green flouorescence (FL1) was collected through a 530/30 band pass filter. The orange fluorescence (FL2) was collected through a 585/42 band pass filter. The red fluorescence (FL3) was collected through a 650 long pass filter. Data acquisition (10^4 events for each sample) was performed using CellQuest software. Photomultiplier tube voltage (set up in linear mode for light scatters and in logarithmic mode for fluorescence with these typical voltages: FL1 = 600, FL2 = 550, and FL3 = 550) and fluorescence compensation (FL1 = Annexin V-FITC, FL2 = TMRM or CMXRos, FL3 = PI) were set up step by step, analyzing cells stained singularly in order to avoid reciprocal interference of the dyes and optimizing the result on samples stained with the three dyes together. As a trigger signal, FSC was used with threshold at channel 100. The order of magnitude of compensation parameters was FL1 -0.5% FL2; FL2 -30% FL1; FL2 -40% FL3; FL3 -40% FL2 for TMRM and FL1 -5% FL2; FL2 -35% FL1; FL2 -55% FL3; FL3 -50% FL2 for CMXRos. The high percentages of compensation between FL2 and FL3 and vice versa were justified by the overlap of emission spectra of CMXRos and PI and TMRM and PI.

Data analysis was performed with WinMDI software. FSC and SSC (both in linear scale), FITC-Annexin V (FL1), CMXRos or TMRM (FL2), and PI (FL3) fluorescent signals were shown as dot plot diagrams. In order to point out the different cell populations, regions were selected on the following dot plots: FSC versus TMRM/CMXRos for cells with normal or depolarized mitochondria (depicted as blue and green dots, respectively); Annexin V versus TMRM/CMXRos for the Annexin V-positive cells (depicted as red dots); and Annexin V versus PI for the Annexin V/PI- positive cells (black dots). To quantify the degree of mitochondrial depolarization, the geometric mean (Gm) of the TMRM signal was calculated on the histogram window of WinMDI after discriminating apoptotic and nonapoptotic subpopulations with a logical gate tool.

RESULTS

Detection of Apoptosis

Human T-leukemia Jurkat cells were exposed to different apoptosis inducers stained with Annexin V-FITC, TMRM, and PI and analyzed. As reported in Figure 1, cells in control conditions responded uniformly with a marked signal to the TMRM staining ($TMRM^+$ cell population; blue dots), indicating a normal inner mitochondrial membrane electrochemical gradient ($\Delta\psi_m$). Only a small percentage of cells, around 5%, showed loss of $\Delta\psi_m$ ($TMRM^-$ cell population; green dots). This cell population was characterized almost entirely by PS exposition on the cell surface (Annexin V^+ cell population; red dots) and altered cell morphology (see the distribution of red dots in the FSC versus SSC plot), thus representing a basal level of cells that undergo apoptosis. Cells positive to the staining with

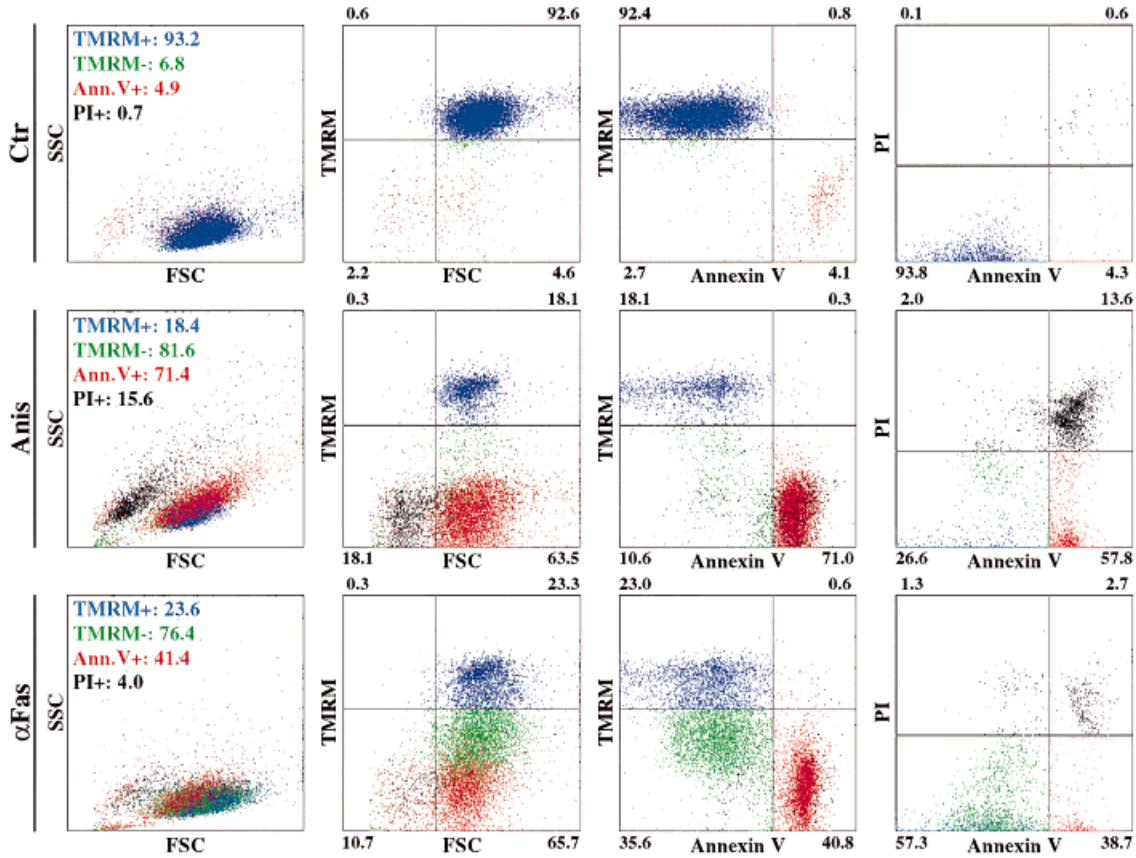

FIG. 1. Measurement of apoptosis induction by multiparametric FACS analysis. Diagrams represent (from left to right): FSC versus SSC analysis; FSC analysis versus TMRM staining; Annexin V-FITC versus TMRM staining; Annexin V-FITC versus PI staining. FSC and SSC parameters are reported on a linear scale and TMRM, Annexin V-FITC, and PI are reported on a logarithmic scale. The percentage of the cell population in each quadrant is indicated. Cells that retain and lose $\Delta\psi_m$ are selected in the upper and lower parts of the FSC versus TMRM plot and are blue and green, respectively. Cells exposing PS on the cell surface are selected in the right quarters of the Annexin V-FITC versus TMRM plot and appear in red. Cells permeable to PI are selected in the upper quarters of the PI versus Annexin V-FITC plot and appear black. The high compensation values are the cause of the compression of data in this last plot. Percentage of each of these cell populations is reported in the top left side of the FSC versus SSC plots. Jurkat cells were exposed for 5 h to 500 ng/ml anisomycin (Anis) or to 150 ng/ml of the CH11 anti-Fas agonist antibody (αFas).

PI, i.e., endowed with a heavily damaged plasma membrane and probably dead, are a negligible percentage (PI^+ cell population; black dots).

Apoptosis was elicited by exposing Jurkat cells to two unrelated compounds, anisomycin, a protein synthesis inhibitor and Jun kinase activator, and the CH11 anti- Fas agonist antibody, which triggers the Fas death pathway following trimerization of the Fas receptor. As depicted in Figure 1, anisomycin delivered a strong apoptotic signal, characterized by a marked $\Delta\psi_m$ breakdown. The majority of cells showing depolarized mitochondria also exposed PS on their cell surface (about 90% of the $TMRM^-$ cells were also Annexin V^+; see also Table 1), whereas some of them were PI^+. Interestingly, the FSC versus SSC plot showed that both Annexin V^+ and PI^+ cells displayed enhanced granularity and cell shrinkage, as indicated by the increase of the SSC parameter and the decrease of the FSC parameter, respectively. These cell changes were highly augmented in the PI^+ cells with respect to the Annexin V^+ cells.

Cell treatment with the anti-Fas antibody caused a marked $\Delta\psi_m$ collapse, but only a part of the $TMRM^-$ cell population exposed PS on the surface (the ratio between Annexin V^+ and $TMRM^-$ cells was about 50%; see also Table 1). These two cell subsets were clearly dis-

Table 1
*Percentage of Cells Displaying High and Low TMRM Staining ($TMRM^+$ and $TMRM^-$ Cell Populations, Respectively), PS Flipping Across the Plasma Membrane (Annexin V^+ Cell Population), and Permeability to PI (PI^+ Cell Population)**

	$TMRM^+$	$TMRM^-$	Annexin V^+	PI^+
Control	93.2 ± 1.3	6.8 ± 1.4	6.5 ± 1.3	1.1 ± 0.4
Anisomycin	21.0 ± 4.6	79.0 ± 4.1	72.2 ± 3.0	10.3 ± 2.2
αFas	21.8 ± 3.8	78.2 ± 3.4	39.1 ± 2.4	4.2 ± 1.4

*Cells were exposed to 500 ng/ml anisomycin or 150 ng/ml CH11 anti-Fas agonist antibody (n = 13 for each condition). Data are shown as mean ± SD and their analysis is performed as in Figure 1.

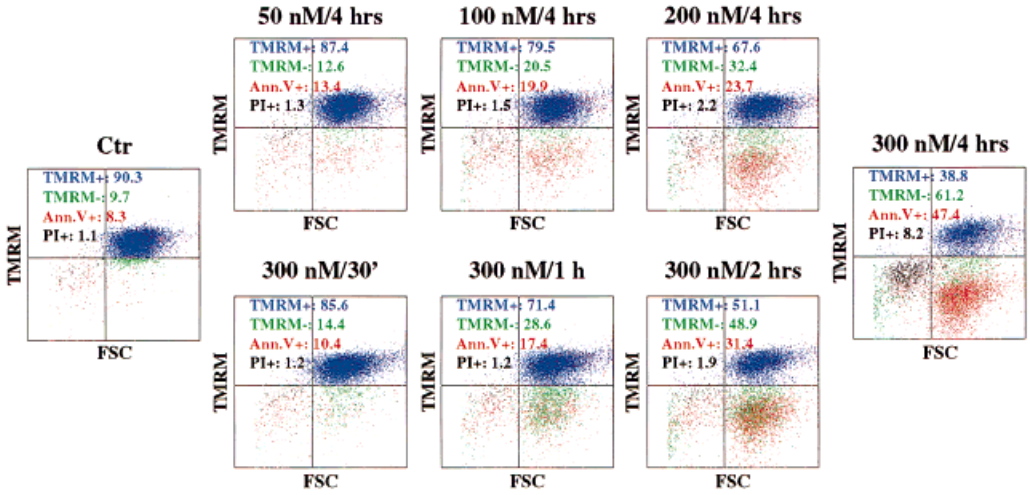

FIG. 2. Dose-response and kinetics analyses of apoptosis induction. Jurkat cells were treated with staurosporine. The drug concentration and time exposure to the drug are reported above each diagram. Data analysis is the same as reported in Figure1, but only the FSC versus TMRM plot is shown. Cell populations are colored and their percentage is reported as in Figure 1.

tinguishable (green and red dots in Fig. 1). Furthermore, plasma membrane integrity was maintained by nearly all cells and cell morphology was not altered dramatically, even though Annexin V^+ cells were not exactly superimposable to the other cell populations in the FSC versus SSC plot. These results were highly reproducible, as is apparent from the low SD values in Table 1.

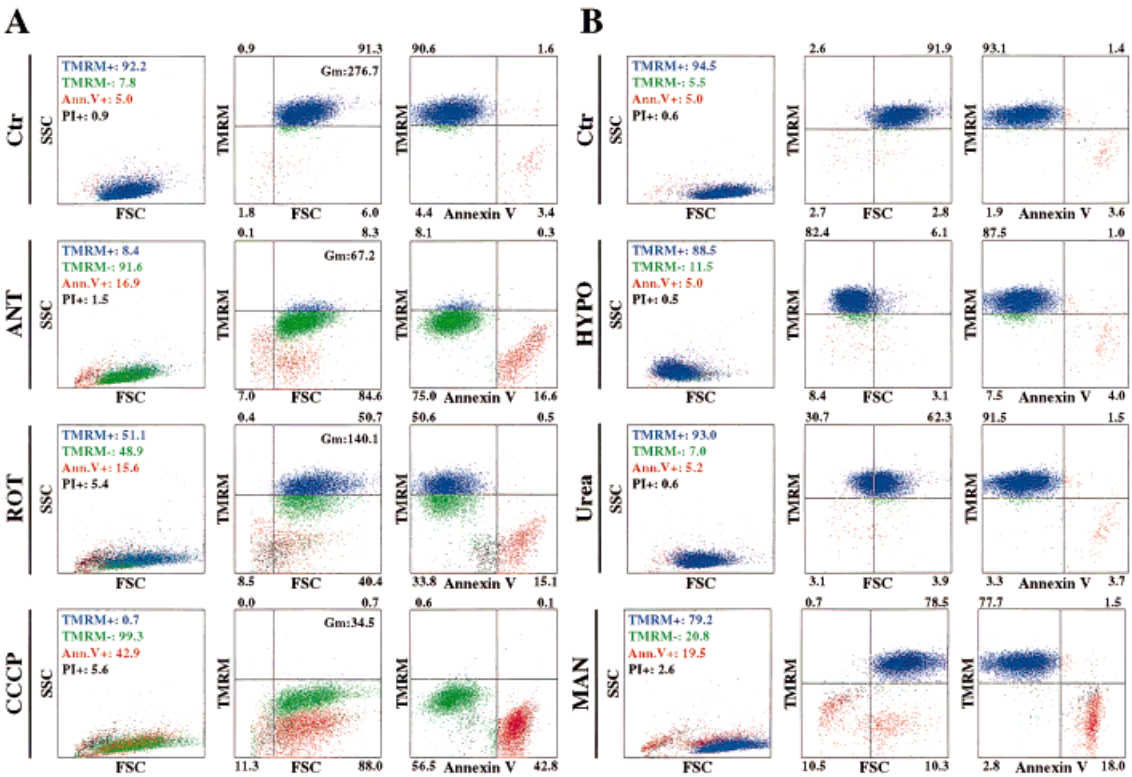

FIG. 3. Effect of mitochondrial depolarizing agents and of anisoosmotic conditions on FACS apoptosis measurements. Jurkat cells were treated for 5 h with **A:** 50 μM antimycin A (ANT), 50 μM rotenone (ROT), or 50 μM CCCP. **B:** A 200-mosM hypotonic solution (HYPO) or 500-mosM hyperosmotic solution was obtained by adding either urea or mannitol (MAN) to the culture medium. Plots are as in Figure 1, but the Annexin V-FITC versus PI diagram is omitted. Cell populations are colored and their percentage is reported as in Figure 1. The Gm values of TMRM staining are displayed in the top left corners of the FSC versus TMRM plots (A).

Dose-Response and Kinetics Analyses of Apoptosis Induction

We assessed the possibility of studying the degree of apoptosis induction and of following step-wise the course of the death process. Jurkat cells were treated with various concentrations of staurosporine, a wide range kinase-inhibitor. As depicted in the upper part of Figure 2, the percentage of cells that underwent each of the apoptotic changes strictly depended on the dose of the agonist used. Furthermore, a time-course analysis displayed a marked $\Delta\psi_m$ breakdown after 1 h of staurosporine treatment (green dots in the lower part of Fig. 2). After 2 h, a cell population appeared that exposed PS on the surface (red dots). Both these subpopulations did maintain a normal cell volume (see the FSC parameter), but the Annexin V^+ cells displayed the lowest TMRM staining. These data suggest a kinetic model in which cells treated with staurosporine enter the apoptotic process by partially depolarizing mitochondria, and then proceed by flipping PS across the plasma membrane and by further collapsing $\Delta\psi_m$. Finally, cells shrink and become permeable to PI (black dots in the plot on the right of Fig. 2).

Control Experiment for the Measure of Mitochondrial Potential and Cell Volume Changes

To test the reliability of the TMRM probe in assessing variations of the inner mitochondrial membrane electrochemical gradient ($\Delta\psi_m$), cells were exposed to three compounds that specifically depolarize mitochondria by different mechanisms. Antimycin A and rotenone block the complex III and I of the respiratory chain, respectively, whereas CCCP uncouples oxidative phosphorylation. As expected, all three drugs were effective in inducing $\Delta\psi_m$ collapse, with an effect on nearly the whole cell population by antimycin A and CCCP and on about one half of the cells by rotenone (Fig. 3A). Interestingly, among $TMRM^-$ cells a subpopulation externalized PS residues, suggesting cell progression toward the activation of an apoptotic program. To better elucidate the degree of $\Delta\psi_m$ loss in each condition, the Gm of the TMRM staining was calculated after cutting off apoptotic and dead cells (Annexin V^+ and PI^+ cell populations). As reported in the top right corners of the FSC versus TMRM plots of Figure 3A, antimycin A, rotenone, and CCCP depolarized mitochondria independently of apoptosis induction (relative $\Delta\psi_m$ values measured as Gm: control, 1.0; rotenone, 0.51; antimycin A, 0.24; CCCP, 0.12). These results indicate that TMRM is an effective dye to measure $\Delta\psi_m$ changes.

To verify the relationship between the FSC parameter and cell volume changes, cells were exposed to anisoosmotic conditions (Fig. 3B). Both a hypoosmotic shock, obtained by adding water to the medium to a final osmolarity of 200 mosM, and a hyperosmotic shock, obtained by adding urea to a final osmolarity 500 mosM, reduced markedly the FSC parameter, without the appearance of any apoptotic feature. The observation that the same effect was obtained on FSC with two osmotic conditions is probably due to the absence of an efficient regulatory volume machinery in lymphocytes (15). Instead, a hyperosmotic shock obtained by the addition of mannitol to the medium caused apoptosis induction, with changes in cell morphology only in the subpopulation undergoing the death process, as we had already described (16).

Comparison between TMRM and CMXRos for the Measure of $\Delta\psi_m$

To measure variations in $\Delta\psi_m$, the TMRM dye was substituted with CMXRos. This probe has been widely used in the past (17), but recent observations cast doubt on the effective reliability of rosamine-derivative probes in assessing $\Delta\psi_m$ loss (18). When we exposed Jurkat cells to anisomycin or the anti-Fas antibody, the result was comparable to that measured with TMRM (compare Figs. 1 and 4A). Some minor differences in the distribution of the subpopulations could be attributed to the high compression of the CMXRos signal on the Y axis. Moreover, the hypoosmotic shock resulted in an almost identical dot plot with CMXRos and TMRM (Figs. 3B and 4A). The same was true for the hyperosmotic shocks with urea and mannitol (not shown). However, when cells were triggered with the specific mitochondrial-depolarizing compounds, no massive breakdown of $\Delta\psi_m$ could be detected, but only the appearance of the $CMXRos^-$/Annexin V^+, i.e., apoptotic, cell population (Fig. 4B). This observation demonstrates clearly that CMXRos is a useful tool to investigate cell populations in a mid-advanced step of the apoptotic pathway, but is ineffective to reveal early or nonapoptotic $\Delta\psi_m$ changes.

DISCUSSION

The causal relationship among morphological and biochemical changes which activate during the apoptotic process is only partially understood. In the present study, we describe the characterization of a simple, reproducible, and accurate technique that allows us to determine, quantify, and integrate several apoptotic events. This assay enables us to study, in one single cell sample, apoptosis induction from its early stages, by analyzing mitochondrial dysfunction, to mid and later steps such as cell volume reduction, PS externalization, and loss of plasma membrane integrity. Others have performed multiparametric flow cytometry analyses to investigate apoptosis (for a review, see ref. 19). However, in some cases, cells were stained separately with different fluorogenic compounds (20,21), or antibodies raised against proteins involved in the apoptotic process were conjugated with fluorophores, and then studied in association with late apoptotic markers (22,23). When several probes were used simultaneously, no early apoptotic steps were investigated (24,25).

This cytofluorometric approach is distinguished from the above reported ones in that it allows the precise and kinetically ordered determination of several apoptotic, or preapoptotic, cell subpopulations. For instance, it was possible to quantify the collapse of $\Delta\psi_m$ and point out a cell subpopulation entering apoptosis after treatment with mitochondrial-depolarizing agents or to discriminate

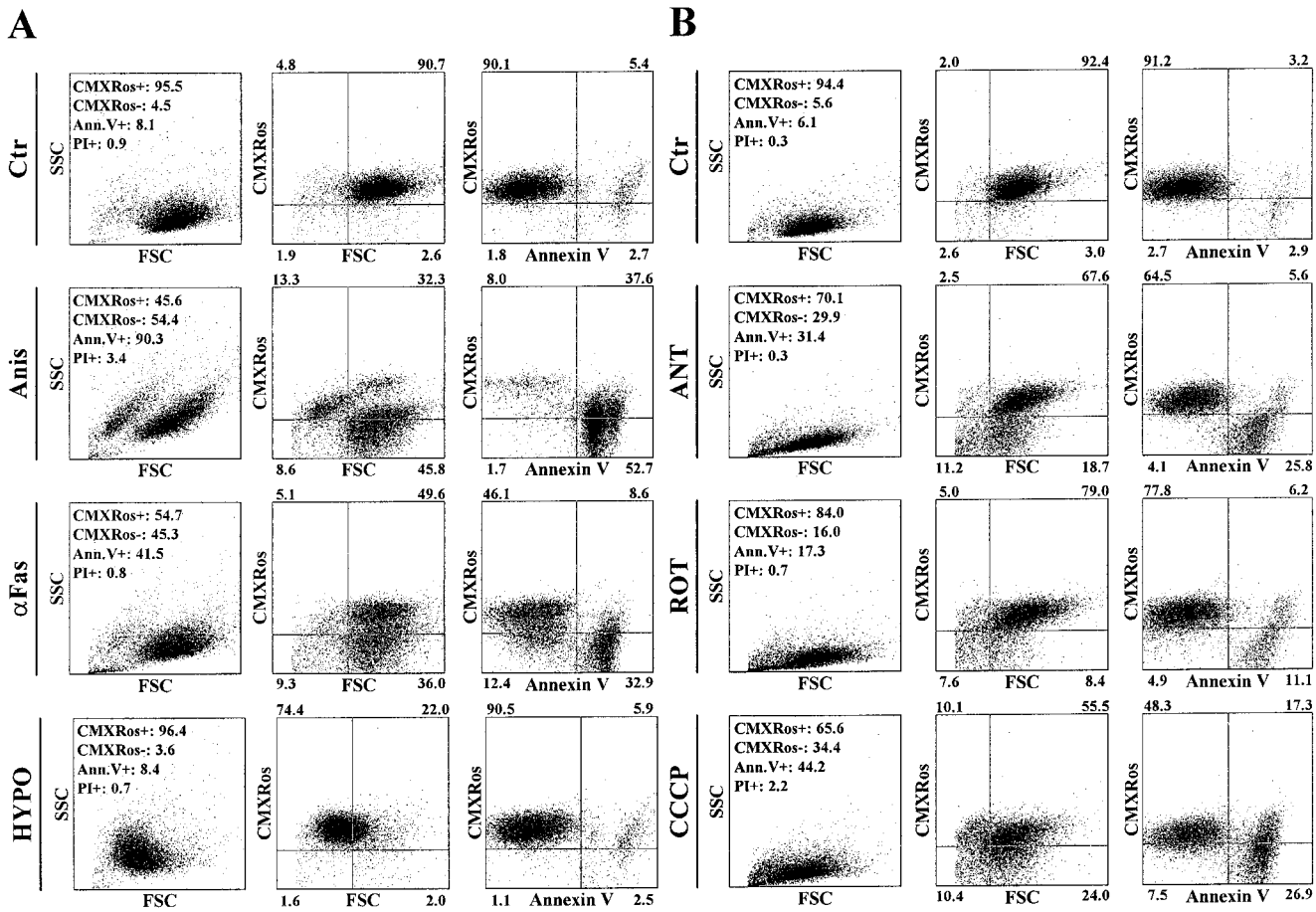

FIG. 4. Use of CMXRos to determine mitochondrial potential in multiparametric FACS analysis of apoptosis induction. Jurkat cells were treated for 5 h with **A:** 500 ng/ml anisomycin (Anis), 150 ng/ml CH11 anti- Fas agonist antibody (αFas), or a 200-mosM hypoosmotic solution (HYPO). **B:** 50 μM antimycin A (ANT), 50 μM rotenone (ROT), or 50 μM CCCP. Plots are as in Figure 3 and the percentage of each cell population is reported as above.

among the effects of different anisoosmotic conditions on cell survival (Fig. 3). Moreover, we discriminated between features of cell subsets undergoing apoptosis induced by unrelated agents such as anisomycin, the anti-Fas antibody, and staurosporine (Figs. 1, 2, Table 1). Indeed, this technique can be a helpful tool to investigate the molecular mechanisms associated with cell death. In this regard, the combined analysis of independent apoptotic features gives additional degrees of information. For example, a cell subpopulation can be described as simultaneously shrunken, granular, with intermediate plasma membrane changes and a marked mitochondrial depolarization. One can study easily the effect of apoptosis modulators, such as caspase inhibitors, calcium chelators, or chemotherapeutic drugs. If associated with time-course analyses (Fig. 2), these experiments could be useful to precisely understand and to order how each pool of cell changes is finely tuned.

Interestingly, the comparison of the two voltage-sensitive, mitochondrion-selective dyes TMRM and CMXRos indicates that the latter needs a higher compensation degree when adjusting flow cytometer parameters (see Materials and Methods). CMXRos does not allow a separation between cells with intact and depolarized mitochondria as good as that achieved with TMRM (compare Figs. 1 and 4A) and more importantly it lacks a complete reliability to measure $\Delta\psi_m$ changes (compare Figs. 3 and 4B). This could be due to a lack of correlation between the magnitude of $\Delta\psi_m$ and the binding of the probe chloromethyl moiety to SH groups inside mitochondria (18). As mitochondria can be considered the central control point of apoptosis (26), it is increasingly important to have a reliable mitochondrial probe.

We only reported data obtained with the human T-leukemia Jurkat cell line. Similar results were collected with several other cell types, such as various T-cell lines, monocytic cell lines, or neutrophils (not shown), indicating the versatility of this technique.

The high accuracy and reproducibility (Table 1) of apoptosis measurements achieved with this multiprobe method could be useful to determine precisely the modulation of this process in pathological samples or in response to pharmacological treatments. For instance, this assay could be used on peripheral blood lymphocyte sam-

ples, in combination with the staining of specific lymphocyte subsets (22), in order to study several lymphoreticular malignancies.

The primary role of the apoptotic process in the control of cell homeostasis and in many diseases highlights the importance of improving methods to better dissect this phenomenon.

ACKNOWLEDGMENTS

We are indebted to Prof. Paolo M. Comoglio and Prof. Federico Caligaris-Cappio for their continuous support and to Dr. Dariush Farahi Far for invaluable discussions. We thank Giovanna Petruccelli and Laura Palmas for technical assistance. A.R. is the recipient of a fellowship of the Istituto Superiore di Sanità, Progetto Finalizzato AIDS.

LITERATURE CITED

1. Budihardjo I, Oliver H, Lutter M, Luo X, Wang X. Biochemical pathways of caspase activation during apoptosis. Annu Rev Cell Dev Biol 1999;15:269–290.
2. Kroemer G, Reed JC. Mitochondrial control of cell death. Nat Med 2000;6:513–519.
3. Ferri KF, Kroemer G. Control of apoptotic DNA degradation. Nat Cell Biol 2000;2:E63–E64.
4. Gross A, McDonnell JM, Korsmeyer SJ. BCL-2 family members and the mitochondria in apoptosis. Genes Dev 1999;13:1899–1911.
5. Strasser A, O'Connor L, Dixit VM. Apoptosis signaling. Annu Rev Biochem 2000;69:217–245.
6. Desagher S, Martinou JC. Mitochondria as the central control point of apoptosis. Trends Cell Biol 2000;10:369–377.
7. Hengartner MO. The biochemistry of apoptosis. Nature 2000;407: 770–776.
8. Loew LM, Tuft RA, Carrington W, Fay FS. Imaging in five dimensions: time-dependent membrane potentials in individual mitochondria. Biophys J 1993;65:2396–2407.
9. Heiskanen KM, Bhat MB, Wang HW, Ma J, Nieminen AL. Mitochondrial depolarization accompanies cytochrome c release during apoptosis in PC6 cells. J Biol Chem 1999;274:5654–5658.
10. Plymale DR, Haskins JR, de la Iglesia FA. Monitoring simultaneous subcellular events in vitro by means of coherent multiprobe fluorescence. Nat Med 1999;5:351–355.
11. Darzynkiewicz Z, Bruno S, Del Bino G, Gorczyca W, Hotz MA, Lassota P, Traganos F. Features of apoptotic cells measured by flow cytometry. Cytometry 1992;13:795–808.
12. Elstein KH, Zucker RM. Comparison of cellular and nuclear flow cytometric techniques for discriminating apoptotic subpopulations. Exp Cell Res 1994;211:322–331.
13. Koopman G, Reutelingsperger CPM, Kuijten GAM, Keehnen RMJ, Pals ST, van Oers MHJ. Annexin V for flow cytometric detection of phosphatidylserine expression on B cells undergoing apoptosis. Blood 1994;84:1415–1420.
14. Vermes I, Haanen C, Steffens-Nakken H, Reutelingsperger C. A novel assay for apoptosis. Flow cytometric detection of phosphatidylserine expression on early apoptotic cells using fluorescein labelled Annexin V. J Immunol Methods 1995;184:39–51.
15. Bortner CD, Cidlowski JA. Absence of volume regulatory mechanisms contributes to the rapid activation of apoptosis in thymocytes. Am J Physiol 1996;271:C950–C961.
16. Rasola A, Farahi Far D, Hofman P, Rossi B. Lack of internucleosomal DNA fragmentation is related to Cl^- efflux impairment in hematopoietic cell apoptosis. FASEB J 1999;13:1711–1723.
17. Macho A, Decaudin D, Castedo M, Hirsch T Susin SA, Zamzami N, Kroemer G. Chloromethyl-X-rosamine is an aldehyde-fixable potential-sensitive fluorochrome for the detection of early apoptosis. Cytometry 1996;25:333–340.
18. Scorrano L, Petronilli V, Colonna R, Di Lisa F, Bernardi P. Chloromethyltetramethylrosamine (Mitotracker Orange) induces the mitochondrial permeability transition and inhibits respiratory complex I. Implications for the mechanism of cytochrome c release. J Biol Chem 1999;274:24657–24663.
19. Darzynkiewicz Z, Juan G, Li X, Gorczyca W, Murakami T, Traganos F. Cytometry in cell necrobiology: analysis of apoptosis and accidental cell death (necrosis). Cytometry 1997;27:1–20.
20. Facompre M, Wattez N, Klura J, Lansiaux A, Bailly C. Relationship between vell cycle changes and variations of the mitochondrial membrane potential induced by etoposide. Mol Cell Biol Res Commun 2000;4:37–42.
21. Ozgen U, Savasan S, Buck S, Ravindranath Y. Comparison of DiOC(6)(3) uptake and annexin V labeling for quantification of apoptosis in leukemia cells and non-malignant T lymphocytes from children. Cytometry 2000;42:74–78.
22. Hasper HJ, Wghorst RM, Richel DJ, Meerwaldt JH, Olthuis FM, Schenkeveld CE. A new four-color flow cytometric assay to detect apoptosis in lymphocyte subsets of cultured peripheral blood cells. Cytometry 2000;40:167–171.
23. Garrido SM, William C, Appelbraun FR, Banker DE. Three-color versus four-color multiparameter cell cycle analyses of primary acute myeloid leukemia samples. Cytometry 2000;42:83–94.
24. Walsh GM, Dewson G, Wardlaw AJ, Levi-Schaffer F, Moqbel R. A comparative study of different methods for the assessment of apoptosis and necrosis in human eosinophils. J Immunol Methods 1998; 217:153–163.
25. Eray M, Matto M, Kaartinen M, Andersson L, Pelkonen J. Flow cytometric analysis of apoptotic subpopulations with a combination of annexin V-FITC, propidium iodide, and SYTO 17. Cytometry 2001; 43:134–142.
26. Desagher S, Martinou JC. Mitochondria as the central control point of apoptosis. Trends Cell Biol 2000;10:369–377.